Tetrahedron 86 (2021) 132086

Contents lists available at ScienceDirect

Tetrahedron

journal homepage: www.elsevier.com/locate/tet

One-pot synthesis of dihydropyridine carboxylic acids via functionalization of 3-((trimethylsilyl)ethynyl)pyridines and an unusual hydration of alkynes: Molecular docking and antifungal activity

Ricardo Ballinas-Indilí [a], Omar Gómez-García [b], Eric Treviño-Crespo [a], Dulce Andrade-Pavón [c, d], Lourdes Villa-Tanaca [d], Ruben A. Toscano [a], Cecilio Álvarez-Toledano [a, *]

[a] Instituto de Química, Universidad Nacional Autónoma de México (UNAM), Circuito Exterior s/n, Ciudad Universitaria, 04510, Ciudad de México, Mexico
[b] Departamento de Química Orgánica, Escuela Nacional de Ciencias Biológicas, Instituto Politécnico Nacional, Prol., de Carpio y Plan de Ayala. Col. Sto. Tomás, 11340, Ciudad de México, Mexico
[c] Departamento de Fisiología, Escuela Nacional de Ciencias Biológicas, Instituto Politécnico Nacional, Av. Wilfrido Massieu S/N Unidad Profesional "Adolfo López Mateos", Zacatenco. Col. Lindavista, CP 07700, Ciudad de México, Mexico
[d] Departamento de Microbiología, Escuela Nacional de Ciencias Biológicas, Instituto Politécnico Nacional, Prol. de Carpio y Plan de Ayala. Col. Sto. Tomás, 11340, Ciudad de México, Mexico

ARTICLE INFO

Article history:
Received 1 February 2021
Received in revised form
11 March 2021
Accepted 12 March 2021
Available online 18 March 2021

Keywords:
Dihydropyridines
Hydration of alkynes
Molecular docking
Antifungal activity
Candida spp

ABSTRACT

Activation of 3-((trimethylsilyl)ethynyl)pyridine with triflic anhydride followed by nucleophilic addition of bis(trimethylsili) ketene acetals and a unusual alkyne hydration allowed to obtain new series of 3-acetylated dihydropyridine acids **3a-h** in a single step. Secondly, docking studies were conducted on four of the test compounds (**3b**, **3e**, **17a** and **17b**) and a reference drug (fluconazole) at the active site of lanosterol 14α-demethylase enzymes (CYP51) from *Candida* spp., *in vitro* inhibition assays were performed with the same compounds and yeast species. Compounds **3b**, **3e**, **17a** and **17b** interacted with key amino acids of the active site of CYP51 enzymes in a similar manner as fluconazole. Compared to fluconazole, the test compounds showed better binding energy values (−4.84 to −9.1 vs. −1.51 to 5.68 kcal/mol) and *in vitro* antifungal activity (lower MIC values) on different *Candida* species. Hence, the dihydropyridine derivatives can be considered candidates for the development of new antifungal drugs.

1. Introduction

The pyridine nucleus is a versatile building block in Organic Synthesis [1,2]. It is intrinsically reactive and susceptible to activation by different agents. For example, the reaction of pyridines with triflic anhydride (Tf_2O) [3], ethyl chloroformate ($ClCO_2Et$) [4], alkyl halides and other electrophiles affords pyridinium salts. The latter display an enhanced electrophilic character in the 4 or 2 position, thus allowing them to react with a variety of nucleophiles [5]. Bis(trimethylsilyl) ketene acetals are nucleophiles that react with pyridinium salts to generate functionalized dihydropyridines. Our group has used such compounds to obtain diverse substituted γ and δ-lactones [6–8].

The common method of preparing 3,4-disubstituted dihydropyridine carboxylic acids involves pyridines with certain substituents (e.g., CO_2Et, CN or CHO) in position 3, which lacks α−hydrogens.5 In the presence of an acetyl group, however, the nucleophilic addition of bis(trimethylsilyl) ketene acetals is not favored. The enolization of the carbonyl group and its subsequent triflation not only activates the aromatic ring, but also sterically hampers the approach of the silylated nucleophile. Consequently, the nucleophilic addition at C-4 is not successful. Therefore, the development of direct methodologies for the preparation of 1,3,4-trisubstituted dihydropyridine carboxylic acids with an enolizable group at C-3 represents a synthetic challenge. Such compounds may be instrumental in the elaboration of more sophisticated

* Corresponding author.
E-mail address: cecilio@unam.mx (C. Álvarez-Toledano).

https://doi.org/10.1016/j.tet.2021.132086
0040-4020/

structures.

On the other hand, fungal infections are a serious and increasingly common problem, especially in hospitals, being the principle cause of morbidity and mortality in immunocompromised patients [9]. Among the particularly problematic fungi are candidiasis, aspergillosis, cryptococcosis and mucormycosis [10,11].

Invasive candidiasis is a serious infection induced by any type of *Candida* yeast. Although *C. albicans* is most frequently responsible for this disease, other species such as *C. glabrata*, *C. dubliniensis*, *C. kefyr*, *C. krusei*, *C. lusitaniae* and *C. parapsilosis* have emerged as important causative agents in recent years [12]. Consequently, a variety of antifungal agents have been developed and classified according to their mechanism of action: inhibitors of ergosterol, nucleic acid, cell wall and microtubule biosynthesis, as well as fungal membrane disruptors [13].

Azole derivatives are the most commonly used antifungal agents [14], but are becoming less effective for treating certain drug resistant *Candida* species [15]. Moreover, the administration of azole derivatives against fungal infections can lead to severe adverse effects, including hepatotoxicity and nephrotoxicity. Hence, it is necessary to design, synthesize and test new antifungal agents that have different structures than those of azoles and other antifungal drugs of choice in clinical practice.

In this sense, recent studies have provided evidence of the antifungal potential of dihydropyridine derivatives in relation to *C. albicans*, *Aspergillus niger* and *A. clavatus.* [16,17] Pyridine derivatives are present in several natural and synthetic compounds with antioxidant, anti-inflammatory, anticancer, antiviral, antihypertensive, antiamoebic, antimalarial and antimicrobial activities [18–20].

The aim of the current study was to synthesize a series of derivatives of trisubstituted dihydropyridines (**3a-h**, **17a** and **17b**), evaluate their antifungal activity against six *Candida* species (*C. glabrata*, *C. dubliniensis*, *C. kefyr*, *C. krusei*, *C. lusitaniae* and *C. parapsilosis*), and perform molecular docking of the derivatives on the active site of the Lanosterol 14α-demethylase (CYP51) enzyme of *Candida* spp. The compounds were synthesized with a novel one-pot methodology, involving the activation of 3-((trimethylsilyl)ethynyl) pyridine, the nucleophilic addition of a series of bis(trimethylsilyl) ketene acetals at the C-4 position, and an unusual hydration of the alkyne moiety. Based on the inhibitory activity against *Candida* species and the docking results, we herein propose the test derivatives as a possible alternative for the treatment of mycosis.

2. Results and discussion

2.1. Chemistry

Dihydropyridine carboxylic acid **3a** was synthesized by the activation of 3-((trimethylsilyl)ethynyl)pyridine **1** with a slight excess (1.2 equiv) of triflic anhydride followed by the nucleophilic addition of 1.2 equiv of the corresponding bis(trimethylsilyl) ketene acetal of structure **2a**. With these conditions, bis(trimethylsilyl) ketene acetal **2a** underwent nucleophilic addition to the C4 position of the pyridinium salt. The subsequent aqueous workup induced the hydration of the alkyne moiety to yield the final product **3a** (Scheme 1). It is remarkable that this one-pot reaction activated the pyridine ring, promoted the nucleophilic addition of the ketene acetal, and favored the hydration of the alkyne in a single step, generating a ketone functionality in position 3.

In order to generalize the method, a series of acids was synthesized by using different bis(trimethylsilyl) ketene acetals, obtaining compounds **3a-h** (Table 1).

The preparation of compounds **3** involved the initial activation of the pyridine ring with triflic anhydride to give a pyridinium salt [2,3]. The latter underwent the nucleophilic addition of bis(-trimethyl) ketene acetal to furnish the dihydropyridine system **6a**. Deprotection of the alkyne by TfO^- afforded the acetylide **7a**, which

Table 1
Synthesized dihydropyridine carboxylic acids **3a-h**.

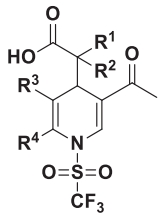

Compound	R^1	R^2	R^3	R^4	Yield (%)
3a	Me	Me	H	H	95
3b	Me	Me	CN	H	48
3c	Me	Me	OMe	H	62
3d	Me	Me	F	H	58
3e	Me	Me	-$(CH)_4$-		78
3f	-$(CH_2)_3$-		–	–	59
3g	-$(CH_2)_4$-		–	–	47
3h	-$(CH_2)_5$-		–	–	80

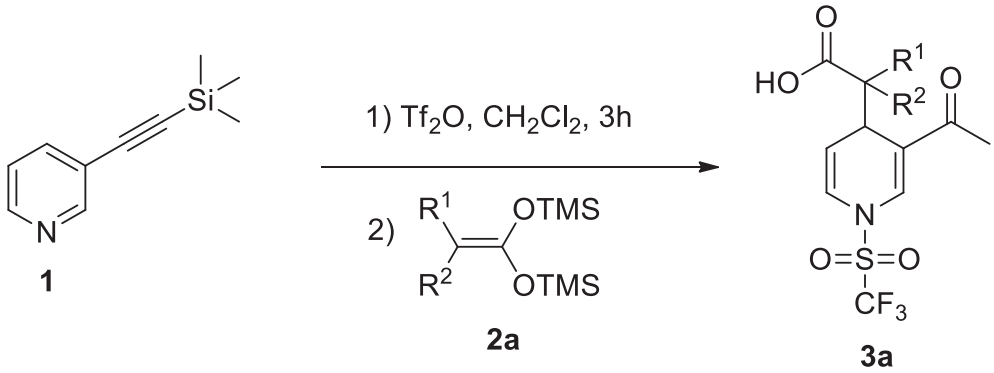

Scheme 1. Synthesis of dihydropyridine carboxylic acid **3a**.

was protonated in the presence of TfOH generated *in situ* during the aqueous workup to provide an alkyne intermediate. Then a reaction with triflic acid through a Markovnikov electrophilic addition led to the carbocation **8a**. The attack of the nucleophilic water molecule on the electrophilic carbocation created an oxonium ion **9a**. This was deprotonated by a triflate to produce the enol **10a**, which was tautomerized to the keto form to obtain compound **3a** (Scheme 2).

It is not possible to attain dihydropyridine derivatives **3** from 3-acetyl pyridine because the carbonyl group becomes enolized and enol triflation occurs. Hence, the presence of the bulky trimethyl silane group blocks the nucleophilic addition of ketene acetal at position 4 of the pyridine ring.

The alkyne hydration that takes place to deliver **3a** is carried out in the absence of Hg reagents, which if utilized are not only highly toxic but also imply a potential risk for escalation, resulting in quite long reaction times [21]. Moreover, the successful route to achieve **3a** does not require the use of expensive transition metals such as Au, Ag, Rh and Ru [22–26].

In the ^{1}H NMR spectra of compounds **3**, the signal at around 3.93–4.62 ppm corresponds to H4 of a dihydropyridine moiety, thus indicating the loss of aromaticity of the pyridine ring as a consequence of the nucleophilic addition of bis(trimethylsilyl) ketene acetal. The signal at 2.10–2.46 ppm was assigned to the acetyl group in position 3, corroborating the hydration of the alkyne group. The ^{13}C NMR spectra display a signal at 179.6–181.9 ppm, ascribed to a carboxylic acid functionality, and a signal at 36.2–5.03 ppm corresponding to C4. The carbonyl signals of the acetyl group between 195.3 and 200.1 ppm and the methyl signals between 24.0 and 25.5 ppm were identified as well, evidencing the conversion of the alkyne to an acyl group. The high resolution mass spectra confirm the presence of the molecular ion in all cases, while the low resolution mass spectra reveal the typical loss of important fragments such as $^{-}$OH and the carboxylic acid fraction. Finally, the molecular structure of **3a** was fully established through an X-ray diffraction analysis (Fig. 1).

The next focus of investigation was the unusual hydration of the alkyne functionality. Reaction of 3-ethynylpyridine **11** under the aforementioned protocol gave **3a** in low yield (23%), demonstrating the importance of the trimethylsilyl group to favor this process (Scheme 3).

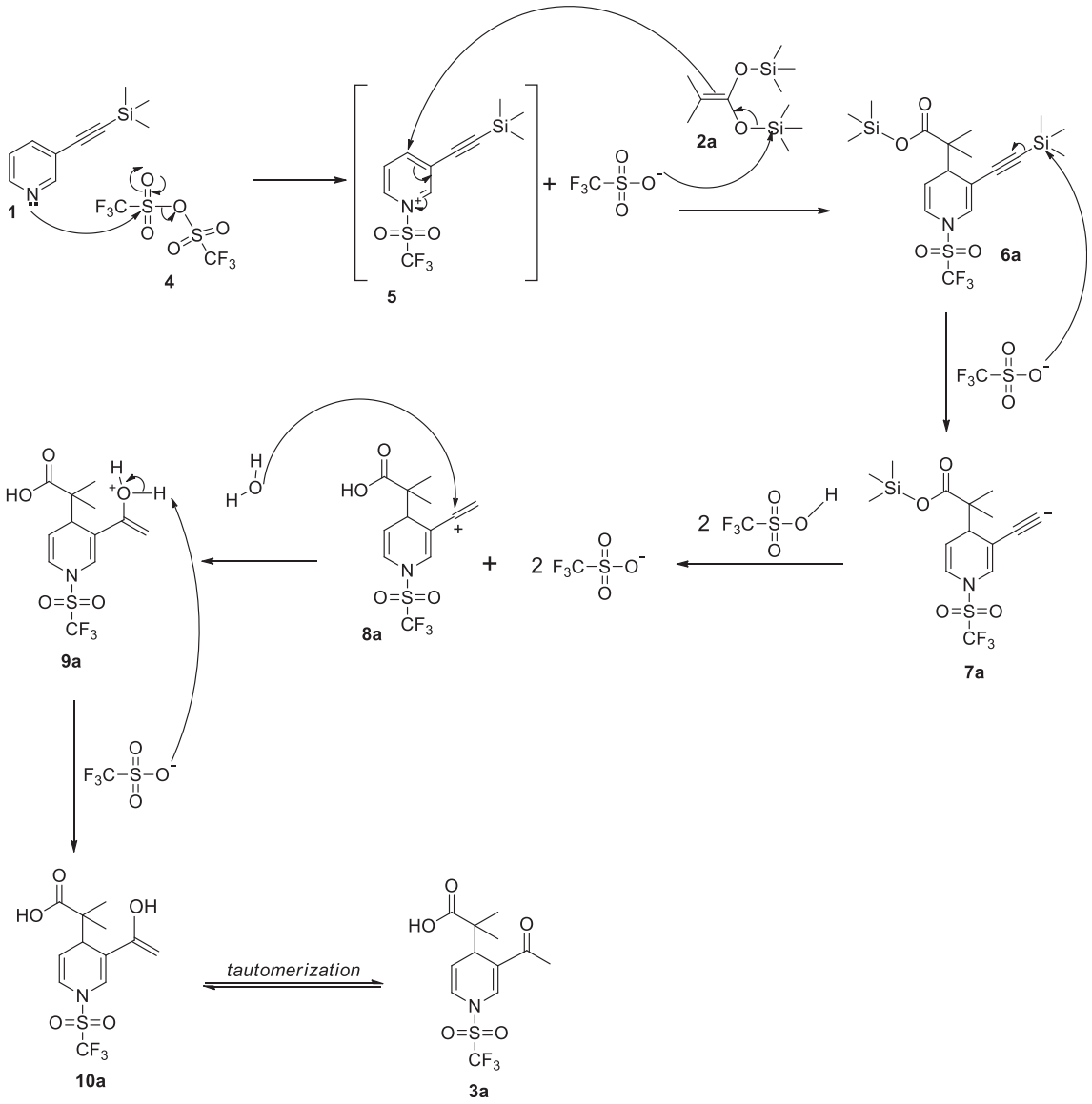

Scheme 2. Proposed mechanism for the formation of compounds **3a-h.**

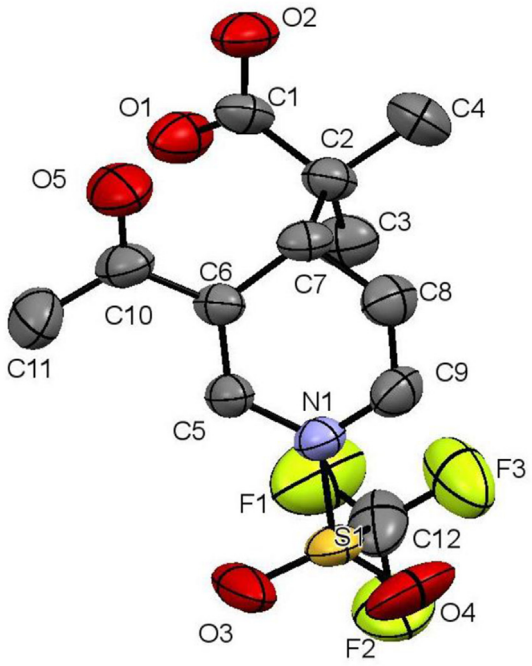

Fig. 1. ORTEP view of compound **3a**. Thermal ellipsoids are shown at the 40% probability level.

The reaction of bis(*tert*-butyldimethylsilyl) ketene acetal **12** also provides **3a** in low yield (28%). This outcome may be attributed to the steric hindrance of the *tert*-butyldimethylsilyl group, which limits the approach of the acetal to the pyridinium salt (Scheme 4).

Further experiments were conducted with alkynes linked to aromatic rings **13** and **14**, resulting in the lack of hydration of the alkyne. Nevertheless, these experiments revealed that Tf_2O is capable of removing the $SiMe_3$ fragment and thereby leaving the alkyne unprotected (Scheme 5).

In another synthetic approach, alkynes with aliphatic or aromatic moieties linked to the triple bond, such as **16a** and **16b**, were reacted under the established protocol. The products were dihydropyridines **17a** and **17b**, with an intact alkyne group. This outcome clearly demonstrates that the $SiMe_3$ group is responsible for the hydration of the alkyne moiety (Scheme 6).

The viability of the isotopic exchange process was also examined in several ways. Firstly, deuterated water was added after the total consumption of the raw material, a process monitored by thin layer chromatography (TLC). The result was a mixture, the mass spectrometry of which exhibited molecular ions with $m/z = 342$, $m/z = 343$ and $m/z = 344$, corresponding to **18**, **19** and **20** of mono-, di- and trideuteration, respectively. The compounds were separated by column chromatography and characterized individually.

When the reaction conditions were varied, using CD_2Cl_2 in the first stage instead of CH_2Cl_2 but with the aqueous workup (as previously described), the same results were obtained. It was possible to identify **3a** and compounds **18**, **19** and **20**. Moreover, the synthetic route was carried out by first employing $CDCl_2$ and then D_2O in a second stage to generate **3a**, **18**, **19** and **20** (see Scheme 7).

In a mechanistic approach to the study, $H_2^{18}O$ was used instead of water in order to corroborate the nucleophilic addition of water on the carbocation **8a** during the hydration of the alkyne. Mass spectrometry showed a molecular ion with $m/z = 344$, confirming the

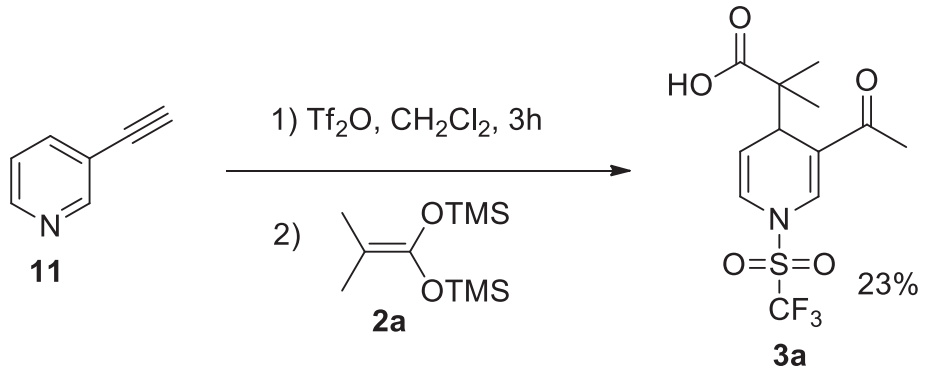

Scheme 3. Synthesis of 2-(3-acetyl-1-((trifluoromethyl)sulfonyl)-1,4-dihydropyridin-4-yl)-2-methylpropanoic acid **3a** from 3-etynil pyridine **11**.

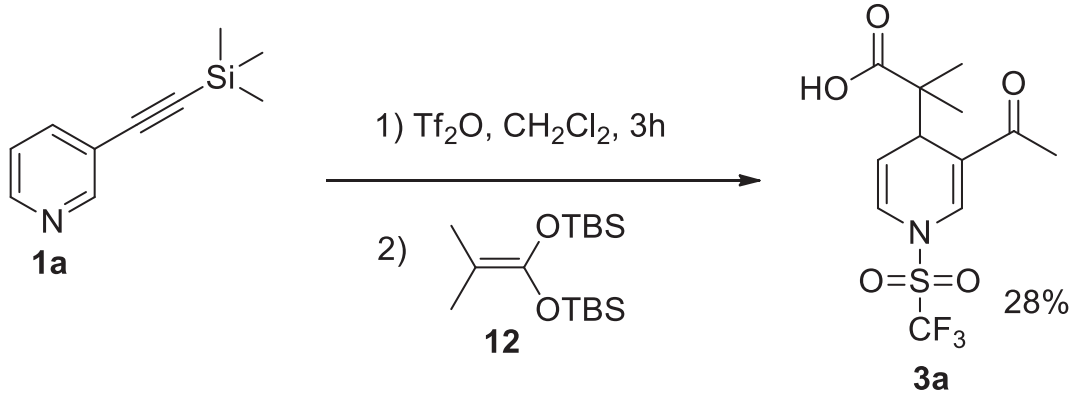

Scheme 4. Synthesis of 2-(3-acetyl-1-((trifluoromethyl)sulfonyl)-1,4-dihydropyridin-4-yl)-2-methylpropanoic acid **3a** using the bis(*tert*-butyldimethylsilyl) ketene acetal **12**.

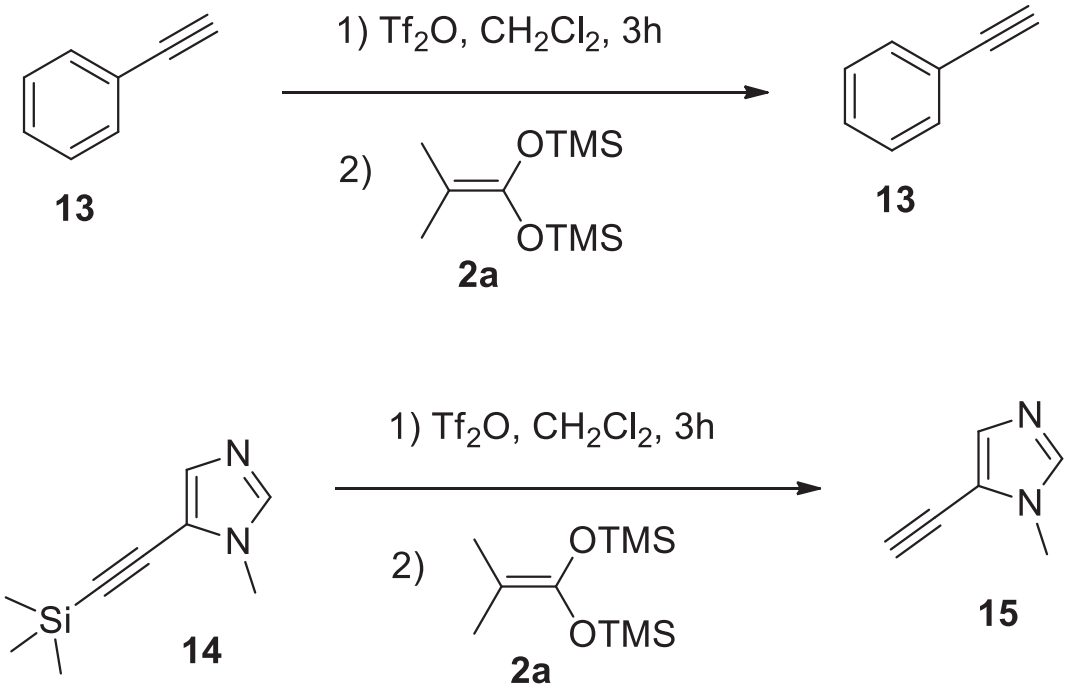

Scheme 5. Reactivity of different alkynes.

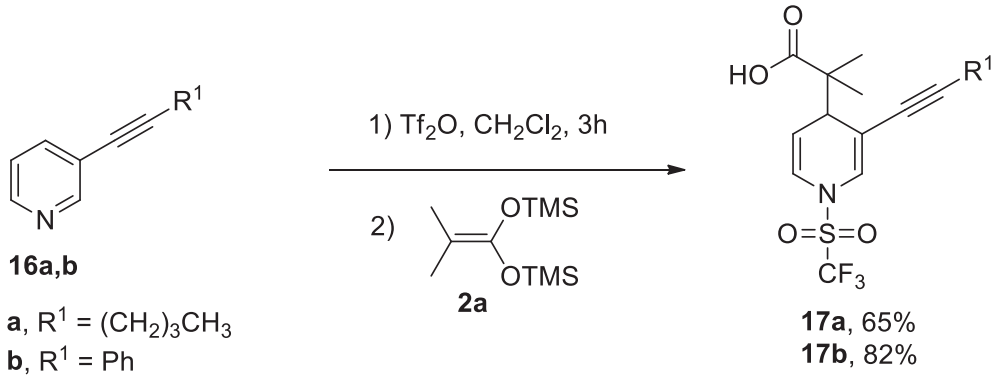

Scheme 6. Synthesis of the dihydropyridine carboxylic acids **17a** and **17b**.

presence of **21** (see Scheme 8).

2.2. Molecular docking of the dihydropyridine derivatives on CYP51 from Candida spp.

To predict the antifungal activity of the dihydropyridine derivatives **3a-h** herein synthesized, a molecular docking study was conducted between some of these compounds and the active site of the CYP51 enzyme from *Candida*. The parameters used to analyze plausible antifungal activity were the binding mode and binding energy of the series of compounds **3** on the CYP51 enzyme. Diverse docking studies have examined potential anti-candidiasis agents in relation to their binding to the CYP51 enzyme, since it is the main target of most antifungal compounds [27–29]. To our knowledge, however, there are no reports of docking studies of dihydropyridine derivatives on this enzyme.

Initially, screening was carried out in order to select the compounds with the best binding energy of the series of dihydropyridine carboxylic acids **3a-h**, **17a** and **17b**. Compounds **3b**, **3e**, **17a** and **17b** showed the best values and were selected for docking simulations and an *in vitro* evaluation of biological activity. The CYP51 enzymes used for docking were those of *C. albicans, C. dubliniensis, C. glabrata, C. krusei, C. lusitaniae* and *C. parapsilosis*. The compounds were selected for their capacity to inhibit *Candida* spp. growth together with their interaction at the active site of the CYP51 enzymes (Fig. 2 and Figs. S1-S5). According to the results, the corresponding derivatives could have a mechanism of action similar to that of azoles (e.g., fluconazole).

The binding energy (Kcal/mol) found for **3b**, **3e**, **17a**, **17b** and fluconazole at the active site of the CYP51 enzymes of *Candida* are listed in Table 2. The four test compounds showed better binding energies (−4.84 to −9.1 kcal/mol) than fluconazole (−1.51 to 5.68 kcal/mol). For four of the CYP51 enzymes, the best binding energies were displayed by **3e** (with a quinoline ring) and **17a**, which may be due to the aromatic benzene ring favoring the interaction with the amino acid side chain at the active site of the enzymes.

The amino acid residues and interactions that participate in

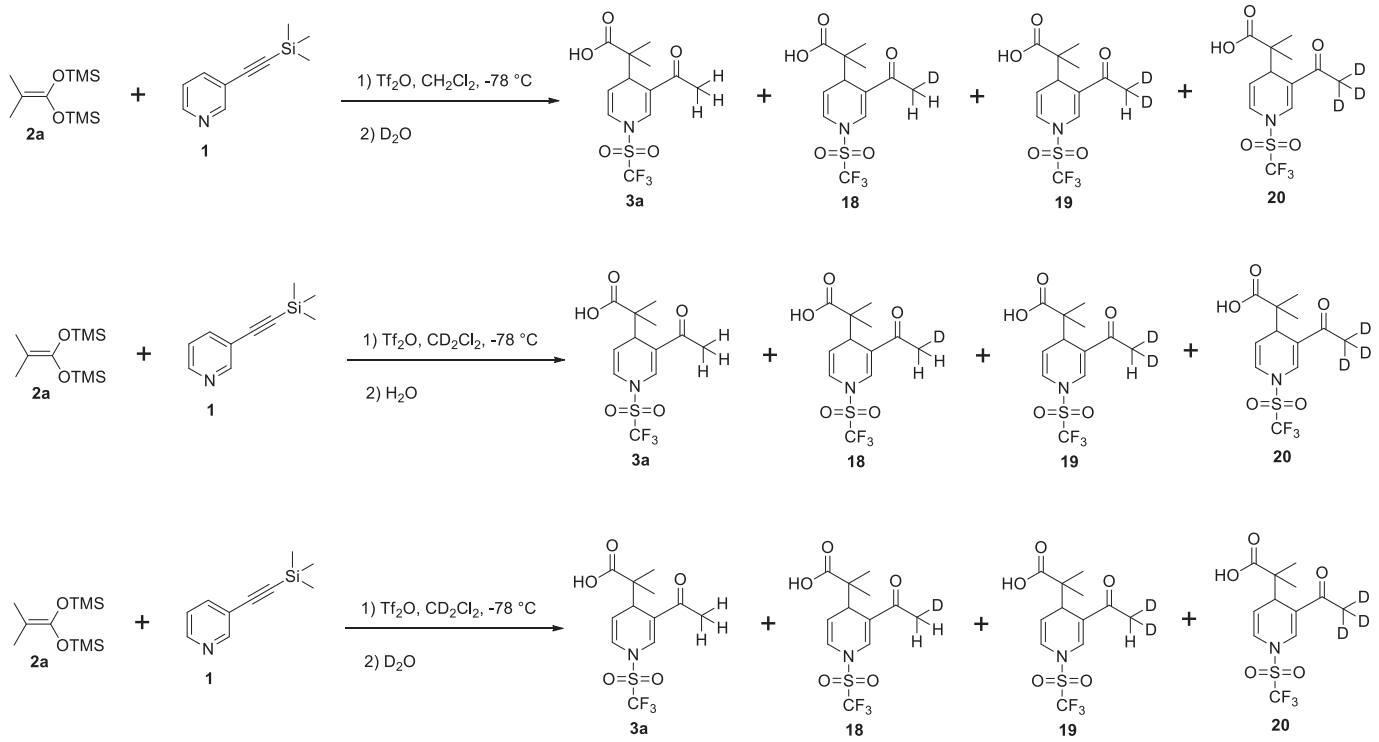

Scheme 7. Deuteration experiments of **3a**.

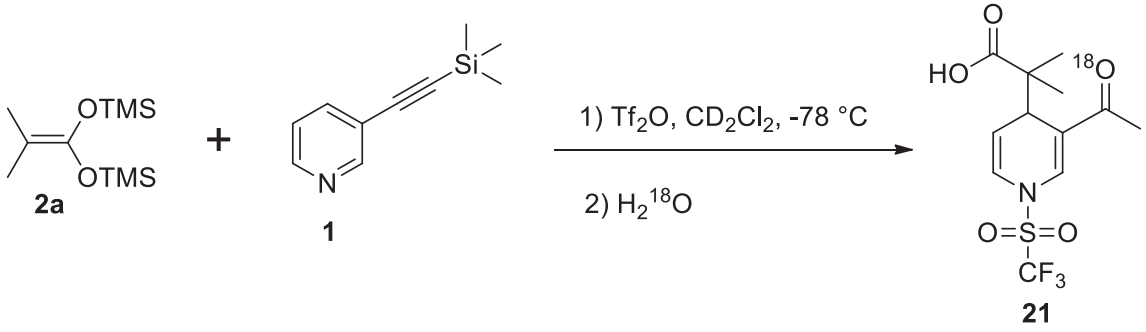

Scheme 8. Hydration of the alkyne with H218O.

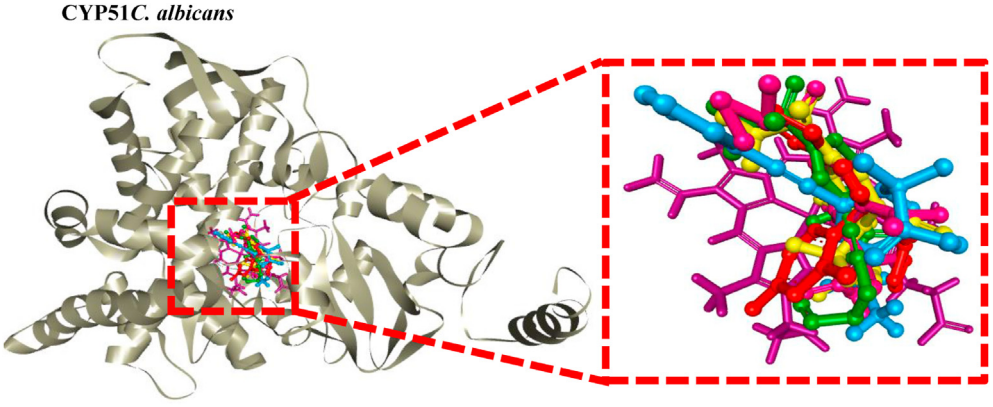

Fig. 2. Binding mode of the selected dihydropyridine derivatives **3b**, **3e**, **17a** and **17b** as well as fluconazole at the active site of CYP51 of *C. albicans*. The protein is portrayed in flat ribbon representation, and the heme group with the stick model (purple). The compounds are illustrated with the ball and stick denotation: fluconazole (red), **3b** (yellow), **3e** (hot pink), **17a** (green) and **17b** (blue).

Table 2
Binding energy from docking simulations of the dihydropyridines **3b**, **3e**, **17a**, **17b** and fluconazole at the active site of CYP51 enzymes of *Candida* spp.

Compounds	Binding Energy (Kcal/mol)					
	C. albicans	*C. dubliniensis*	*C.glabrata*	*C.krusei*	*C.lusitaniae*	*C.parapsilosis*
Fluconazole	−4.44	−4.56	−4.38	−5.68	−5.16	−1.51
3b	−8.66	−7.46	−8.23	−7.82	−8.18	−0.29
3e	−9.83	−8.32	−8.28	−9.1	−9.44	−1.19
17a	−7.6	−8.06	−7.52	−9.0	−8.75	−4.84
17b	2.53	−8.98	−7.96	−8.72	−9.05	2.79

Table 3
Data from the docking of the dihydropyridines on CYP51 enzymes of *Candida* spp.

Compounds	amino acid residues	hydrophilic interactions	hydrophobic interactions
CYP51 *C. albicans*			
Fluconazole	Tyr94, Leu97, Thr98, Phe102, Ile107, Tyr108, Phe204, Met282, Gly283, Gly284, Thr287, Leu352, Ile355, Met484, Val485	C—H ….O (Tyr108) C—H ….O (Gly283) N ….H—O (Thr287)	π-π T-shaped Tyr94 π-alkyl Leu352 π-alkyVal485
3e	Tyr94, Leu97, Thr98, Phe102, Tyr108, Phe204, Met282, Gly283, Gly284, Thr287, Leu352, Met484, Val485	O—H ….O (Tyr108) O ….H—N (Thr287)	π-sigma Tyr94 Halogen Met282 π-alkyl Leu352
CYP51 *C. dubliniensis*			
Fluconazole	Tyr94, Thr98, Phe102, Tyr108, Phe204, Gly279, Met282, Gly283, Gly284, Thr287, Leu352, Val485	C—H ….O (Tyr108) C—H ….O (Met282) N ….H—C (Gly283) O—H ….O (Gly283)	π-π T-shaped Tyr94 Halogen Gly279 Halogen Gly283 π-alkyl Val485
17b	Tyr94, Thr98, Phe102, Val106, Ile107, Tyr108, Phe204, Gly279, Ile280, Gly283, Thr287, Leu352, Met484, Val485	O—H ….O (Tyr108)	π-anion Tyr94 π-alkyl Tyr94 π-π T-shaped Phe102 π-alkyl Ile107 Halogen Met484 π-alkyl Leu352
CYP51 *C. glabrata*			
Fluconazole	Tyr108, Phe116, Ile121, Tyr122, Phe218, Phe223, Gly296, Thr300, Leu362, Leu365, Met493	C—H ….O (Tyr122)	π-π T-shaped Tyr108 π-alkyl Ile121 Halogen Gly296 π-alkyl Leu362
3e	Tyr108, Phe116, Ile121, Tyr122, Phe218, Met295, Gly296, Gly297, Thr300, Pro361, Leu362, Leu365, Met493, Val494	O—H ….O (Met295) O ….H—O (Thr300)	π-π T-shaped Tyr108 π-alkyl Leu362
CYP51 *C. krusei*			
Fluconazole	Tyr94, Leu97, Phe102, Tyr108, Phe199, Ile207, Gly273, Val274, Gly277, Gly278, Thr281, Leu344, Ile347, Met478	C—H ….O (Tyr108) N ….H—N (Gly277) N ….H—O (Gly281)	π-π T-shaped Tyr94 π-π T-shaped Phe102 π-alkyl Leu344
3e	Tyr94, Leu97, Phe102, Ile207, Tyr108, Phe199, Gly273, Val274, Met276, 8Gly277, Gly278, Thr281, Leu344, Ile347, Met478	F ….H—N (Gly277) F ….H—N (Gly278)	π-sigma Tyr94 Halogen Gly273 π-π T-shaped Gly277
CYP51 *C. lusitaniae*			
Fluconazole	Tyr94, Thr98, Ile107, Tyr108, Leu115, Gly283, Gly284, Thr287, Leu352, Ile355, Met481	O—H ….O (Tyr108) F ….H—O (Thr287)	π-π T-shaped Tyr94 π-sigma Ile107 Halogen Gly283 π-alkyl Leu352
3e	Tyr94, Leu97, Thr98, Ile107, Tyr108, Gly279, Val280, Gly283, Thr287, Leu352, Met481		
CYP51 *C. parapsilosis*			
Fluconazole	Tyr94, Tyr108, Phe204, Arg274, Phe333, Gly336, Pro382, Met428, Arg337		Halogen Arg274 Halogen Arg337
17a	Phe102, Phe204, Arg274, Gly275, Val278, Phe333, Arg337, Met428, Val429	O ….H—N (Arg337)	π-sigma Phe204 π-alkyl Val278 π-alkyl Phe333 Halogen Phe333

binding are summarized in Table 3. The following residues of the active site of the CYP51 enzymes are involved in the majority of interactions with fluconazole and the four test compounds (**3b**, **3e**, **17a** and **17b**): Tyr94, Thr98, Phe102, Tyr108, Phe204, Gly283, Gly284 and Thr287 (see Table 4).

The 3D and 2D portrayal of the interactions of the test compounds and reference drug with the CYP51 enzymes of the *Candida* species herein evaluated are shown in Fig. 3 and S6-11. In the 3D

Table 4
MIC for the dihydropyridine derivatives and the reference drug, calculated from *in vitro* antifungal assays against *Candida* spp.

Compounds	MIC μg/μL					
	C. albicans	*C. dubliniensis*	*C. glabrata*	*C. krusei*	*C. lusitaniae*	*C. parapsilosis*
Fluconazole	16	8	16	32	>64	4
3b	10	10	10	10	10	10
3e	10	10	10	20	10	10
17a	10	10	10	10	5	2.5
17b	10	5	10	10	10	10

diagrams, the surface involved in the interaction and the corresponding amino acids can be appreciated. On the other hand, the 2D illustration reveals the type of interactions between the compounds and CYP51.

Several hydrophilic interactions were identified, such as hydrogen bonds formed between fluconazole and the Tyr108 residue in *C. albicans*, *C. dubliniensis* and *C. krusei*. Conventional hydrogen bonds were found between Tyr108 of *C. albicans* and the dihydroquinoline derivative **3e**. This same amino acid residue in *C. lusitaniae* interacts with fluconazole. In *C. albicans* and *C. dubliniensis*, Gly283 is an important fragment that interacts with fluconazole. Interestingly, both **3e** and fluconazole share a conventional hydrogen bond interaction with Thr287 from *C. albicans* and with Gly277 from *C. krusei*. Similar interactions have been reported between CYP51 and other pyrimidine derivatives [27].

Meanwhile, the analysis of hydrophobic interactions revealed which amino acids participate in type π-alkyl non-polar interactions: Tyr94, Phe333, Leu344, Leu352, Val485, π-π T-shaped (Tyr94, Phe102 and Thr108), π-sigma (Tyr94, Ile107 and Phe204) and halogen (Gly273, Arg274, Gly279, Met282, Gly283, Gly296, Phe333, Arg337 and Met484). Moreover, the heme group of the CYP51 enzymes of the *Candida* species herein considered interacts with fluconazole and **3e** through their aromatic fraction, presenting π-π stacked and π-π T-shaped interactions. Finally, the CF_3 group of some derivatives formed halogen bonds with amino acid residues such as Gly273, Met282, Gly296 and Met484.

The interaction between the aforementioned residues and various compounds has been described in previous reports [27–29]. Thus, the current findings of the interaction of **3b** and **3e** with the same residues indicates that their probable mechanism of action is the inhibition of the CYP51 enzyme in each species of *Candida* yeast herein examined.

2.3. Antifungal Activity

The compounds were tested *in vitro* for antifungal activity on the presently considered *Candida* species, determining the minimum inhibitory concentration (MIC). The results corroborate the data on binding energy from the docking simulations. As was found with the binding energy values, the MIC values were better for the dihydropyridine derivatives than fluconazole. Each of the compounds had a MIC of 10 μg/mL for most *Candida* spp., with the best MIC (2.5 μg/mL) corresponding to **17a** applied to *C. parapsilosis*. The MIC values are lower than those obtained in other studies with similar derivatives [30–36], revealing a greater inhibitory effect of the proposed compounds on the *Candida* species herein evaluated.

Compound **3e** showed the lowest MIC for *C. albicans* and the lowest binding energy for *C. dubliniensis*. Derivative **17a** displayed the lowest MIC for *C. parapsilosis* and **17b** for *C. dubliniensis*. These results suggest that the dihydropyridine derivatives probably all have a similar mechanism of inhibition of the CYP51 enzyme.

Based on their MIC values and affinity for the CYP51 enzyme, compounds **3b** and **3e** proved to be promising candidates for further testing as alternative antifungal treatments. Their likely mechanism of action is the inhibition of yeast growth by binding to the active site of CYP51 of *Candida* species.

3. Conclusions

A new series of dihydropyridine carboxylic acids were synthesized through a one-pot process involving the activation of 3-((trimethylsilyl)ethynyl)pyridine with triflic anhydride, followed by the nucleophilic addition of bis(trimethylsilyl) ketene acetals, and finally an unusual alkyne hydration. The advantage of this method over current methodologies for the hydration of alkynes is that it does not require Hg reagents or expensive transition metals. According to the docking results, the dihydropyridine derivatives **3b**, **3e**, **17a** and **17b** interact with key amino acid residues at the active site of CYP51 enzymes of *Candida* species, evidencing a mechanism of action similar to the reference drug (fluconazole). Compared to fluconazole, **3b**, **3e**, **17a** and **17b** showed better binding energy values and therefore greater affinity for the active site of CYP51 of *C. albicans*, *C. dubliniensis*, *C. glabrata*, *C. krusei, C. lusitaniae* and *C. parapsilosis*. The *in vitro* assays carried out to evaluate the inhibition of the *Candida* species revealed lower MIC values for the dihydropyridines than fluconazole. As can be appreciated, **3b**, **3e**, **17a** and **17b** are promising compounds for the treatment of mycosis and should certainly be of value as lead compounds for the development of new antifungal drugs.

4. Experimental section

4.1. General information

All reagents and solvents were of analytical grade, acquired from commercial suppliers and used without further purification. Melting points were measured on a Melt Temp II apparatus. The IR spectra were recorded on a Bruker TENSOR 27 spectrophotometer, and the ^{1}H and ^{13}C NMR spectra on a Bruker Advance III apparatus at 300 MHz and 75 MHz, respectively, in chloroform-*d*. Chemical shifts are given in ppm with reference to TMS. MS-DART spectra were obtained with a JEOL JMS-T100LC spectrometer.

Suitable crystals of **3a** were grown in a hexane/acetone system for a more detailed scrutiny of its molecular structure with X-ray diffraction. The crystal was placed on fiberglass at 25 °C and then put in a Bruker Smart Apex CC diffractometer equipped with Mo radiation ($\lambda_{MoK\alpha} = 0.71073$ Å). The decay was negligible in all cases. Systematic absences and intensity statistics were employed for space group determination. The structure was established with direct methods on the SHELXS-2013 program. The solution and refinement of structures were performed with SHELXL-2013.The refinements of the anisotropic structure were made with the least squares technique for all non-hydrogen atoms. The hydrogens were placed in idealized positions based on their hybridization with isotropic thermal parameters fixed at 1.2 times the value of the attached atom. The different acetals of bis(trimethyl) silyl ketene

CYP51 *C. albicans*-fluconazole

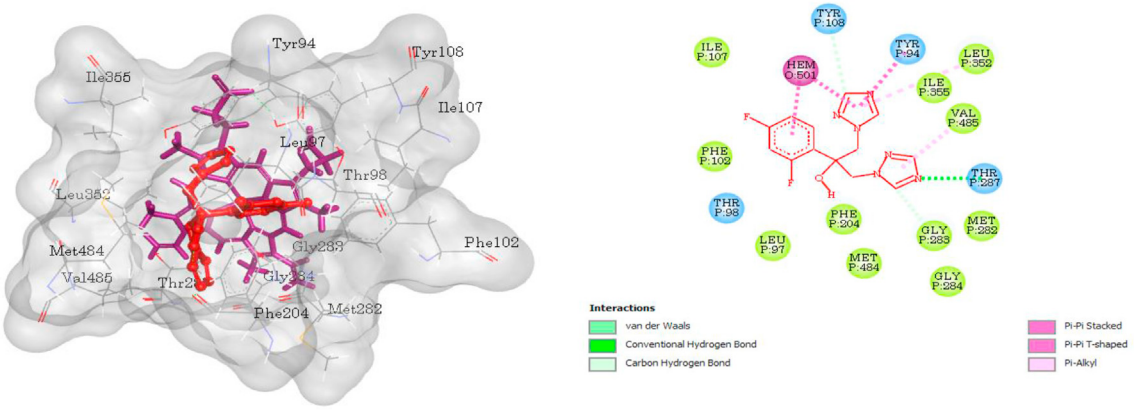

CYP51 *C. albicans*-3b

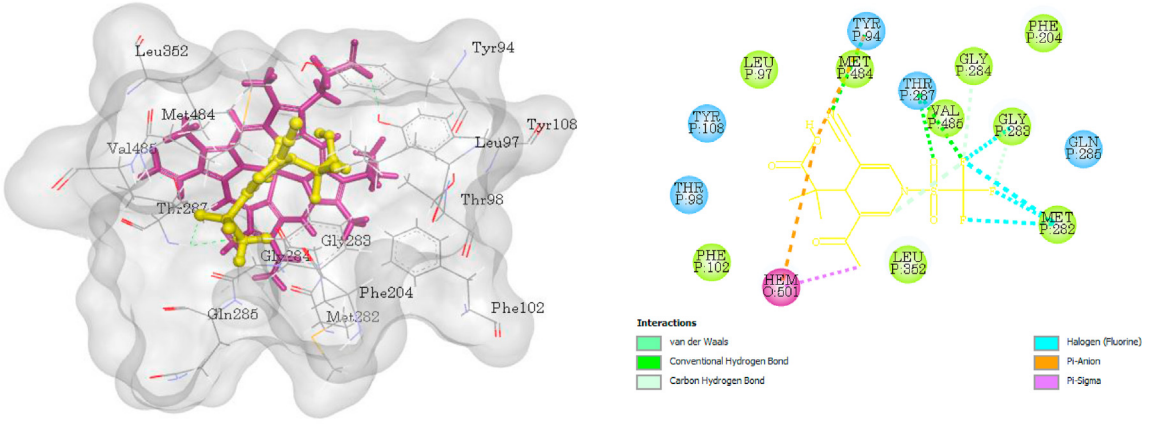

CYP51 *C. albicans*-3e

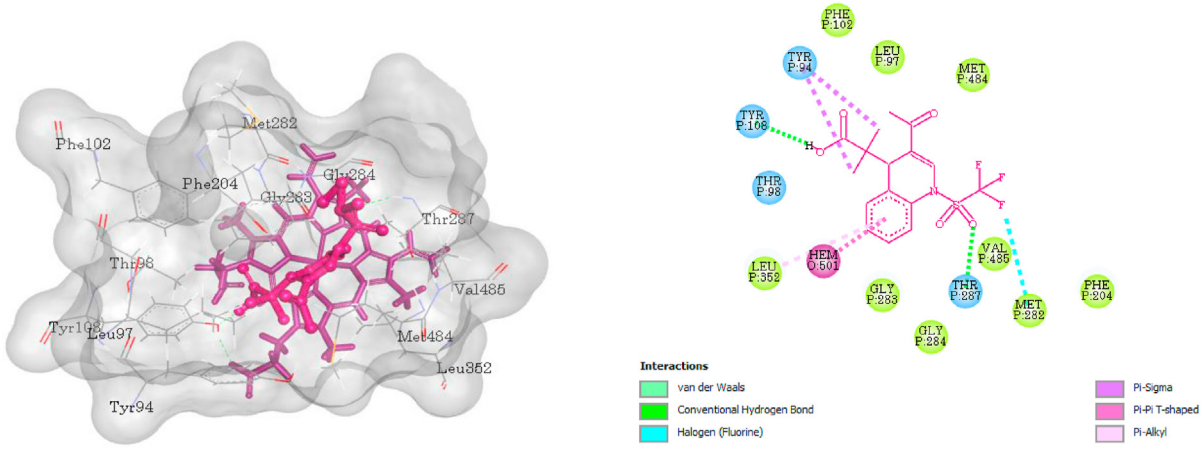

Fig. 3. Molecular interactions of selected dihydropyridine derivatives (**3b** and **3e**) and fluconazole with the active site of CYP51 of *C. albicans*. The surface and slab are illustrated in the 3D structure. The heme group is shown in stick representation (purple), while the compounds are portrayed in ball and stick representation: fluconazole (red), **3b** (yellow) and **3e** (hot pink). The 2D structure depicts the participating interactions on the right side of the figure.

2a-e were prepared according to methods reported in the literature [37].

4.2. General procedure for the synthesis of ((trimethylsilyl)ethynyl) pyridine derivatives

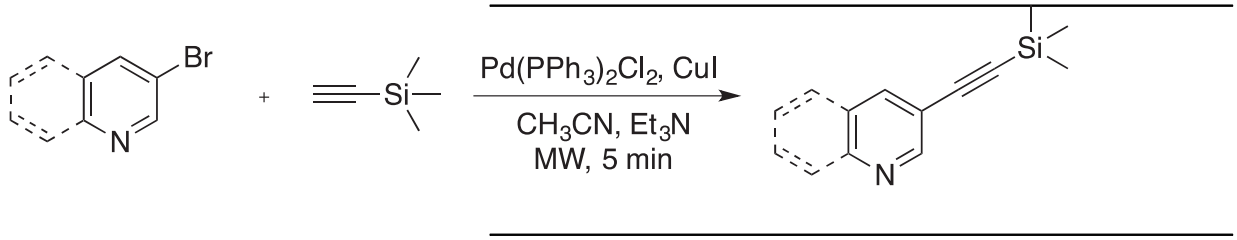

The starting materials pyridine and quinoline derivatives were prepared following the reported procedure [38]. A sealed 10 mL glass tube containing bromopyridine derivative 0.24 g (1.5 mmol), trimethylsilylacetylene (1.5 mmol), triethylamine (7.5 mmol), $Pd(PPh_3)_2Cl_2$ (5 mol %), CuI (10 mol %), and acetonitrile (2 mL) was placed in the cavity of a microwave reactor and irradiated for 5 min, at 120 °C and power 150 W. After cooling to room temperature by an airflow, the tube was removed of the reactor. The reaction mixture was extracted with dichloromethane (30 mL) and water (30 mL). The organic layer was separated and washed with water (2 × 30 mL), dried over anhydrous sodium sulfate, and concentrated under vacuum. Purification by column chromatography, using hexane: ethyl acetate as elution system gave ((trimethylsilyl) ethynyl)pyridine derivatives as colored oils or solids. All the products were characterized.

4.3. General procedure for the synthesis of dihydropyridine carboxylic acids ***3a-h***

To a solution with 0.3g (1.76 mmol) 3-((trimethylsilyl)ethynyl) pyridine dissolved in 15 mL of anhydrous CH_2Cl_2 (under inert atmosphere and cooled to −78 °C), 0.36 mL (2.12 mmol, 1.2 equiv) of triflic anhydride were added with a syringe, and the mixture was stirred constantly for 3 h. Subsequently, 2.12 mmol (1.2 equiv) of the corresponding ketene acetal were added and stirring continued at −78 °C for 2 h. The reaction was then allowed to reach 25 °C before being transferred to a separatory funnel and washed with water (3 × 30 mL). The organic phases were combined and dried with anhydrous Na_2SO_4, and the solvent was removed by vacuum evaporation. The reaction crude was purified by column chromatography using silica gel with hexane/AcOEt mixtures as eluents to obtain the title compounds **3a-h**.

4.3.1. 2-(3-acetyl-1-((trifluoromethyl)sulfonyl)-1,4-dihydropyridin-4-yl)-2-methylpropanoic acid (***3a***)

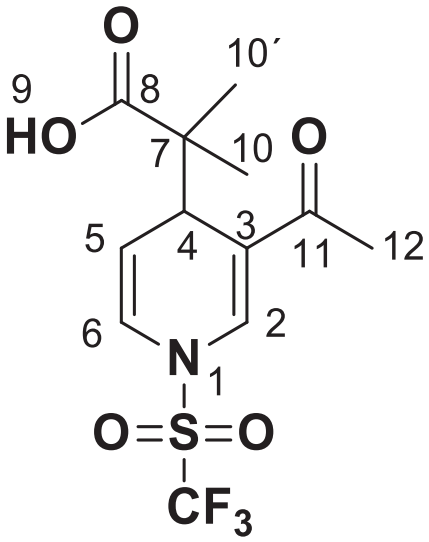

The compound was obtained as a white solid. mp. 92−94 °C, (0.49 g, 85%). IR ν_{max} (KBr): 3512, 3123, 2982, 1707, 1676, 1233 cm^{-1}. ^1H NMR ($CDCl_3$, 300 MHz); δ = 12.2 (s, H-9), 7.59 (s, 1H, H-2), 6.73 (d, J = 7.5 Hz, 1H, H-6), 5.45 (dd, J = 7.5, 6.0 Hz, 1H, H-5), 4.1 (d, J = 6.0 Hz, 1H, H-4), 2.39 (s, 3H, H-12), 1.14 (s, H-10), 1.06 (s, H-10′) ppm. ^{13}C NMR ($CDCl_3$, 75 MHz); δ = 196.8, 182.1, 132.5, 122.7, 122.5, 119.1 (J = 321.0 Hz, CF_3), 111.8, 47.4, 37.8, 25.2, 21.6, 20.4 ppm; MHRMS: calcd for $C_{12}H_{15}F_3NO_5S$ 342.0623, found 342.0500.

*4.3.2. 2-(3-acetyl-5-cyano-1-((trifluoromethyl)sulfonyl)-1,4-dihydropyridin-4-yl)-2-methylpropanoic acid (**3b**)*

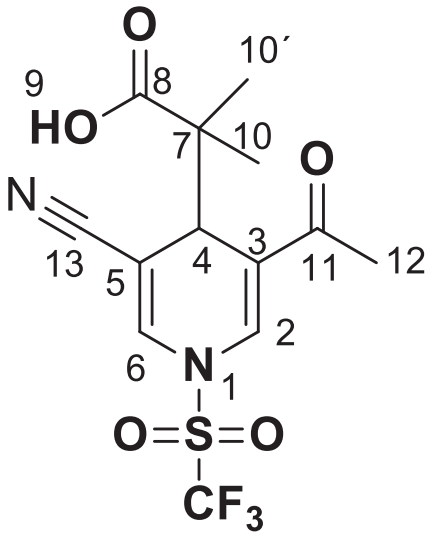

The compound was obtained as a white solid. mp. 110–112 °C, (0.30 g, 48%). IR ν_{max} (KBr): 3431, 3105, 2965, 1705, 1651, 1424, 1242, 1127 cm^{-1}. ^1H NMR (Acetone-d_6, 300 MHz): $\delta = 7.88$ (d, $J = 2.1$ Hz, 1H, H-2), 7.28 (t, $J = 1.2$ Hz, 1H, H-6), 4.03 (s, 1H, H-4), 2.06 (s, 3H, H-12), 1.35 (s, 3H, H-10), 1.27 (s, 3H, H-10′) ppm. ^{13}C NMR (Acetone-d_6, 75 MHz); δ = 185.6, 175.4, 151.4, 145.0, 136.1, 123.7, 119.1 ($J = 321.0$ Hz, CF_3), 116.6, 106.0, 48.7, 22.5, 20.4 ppm. HRMS: calcd for $C_{13}H_{14}F_3N_2O_5S$; calculated 367.0575, found 367.0724.

*4.3.3. 2-(3-acetyl-5-methoxy-1-((trifluoromethyl)sulfonyl)-1,4-dihydropyridin-4-yl)-2-methylpropanoic acid (**3c**)*

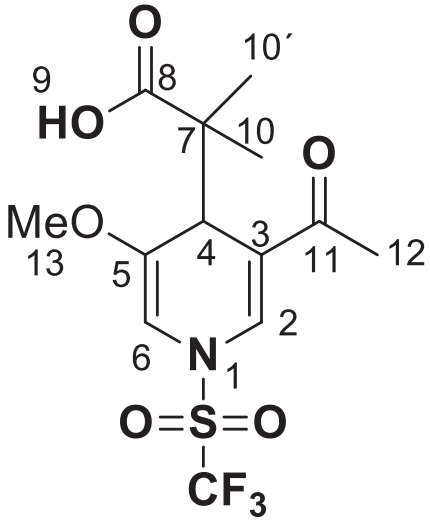

The compound was obtained as a white solid. mp. 100–102 °C, (0.38 g, 62%). IR ν_{max} (KBr): 3458, 3111, 2958, 1762, 1637, 1418, 1203 cm^{-1}. ^1H NMR ($CDCl_3$, 300 MHz): $\delta = 12.35$ (s, 1H, H-9), 6.99 (s, 1H, H-2), 6.10 (s, 1H, H-6), 3.83 (s, 1H, H-4), 3.36 (s, 3H, OCH_3), 2.31 (s, 3H, H-12), 0.93 (s, 3H, H-10), 0.84 (s, H-10′) ppm. ^{13}C NMR ($CDCl_3$, 75 MHz); δ = 191.9, 177.2, 145.6, 132.0, 129.1, 124.6, 120.9 ($J = 321.0$ Hz, CF_3), 105.7, 100.55, 56.8, 51.7, 46.1, 23.0, 22.3 ppm. HRMS: calcd for $C_{13}H_{17}F_3NO_6S$; calculated 372.0728, found 372.0781.

*4.3.4. 2-(3-acetyl-5-fluoro-1-((trifluoromethyl)sulfonyl)-1,4-dihydropyridin-4-yl)-2-methylpropanoic acid (**3d**)*

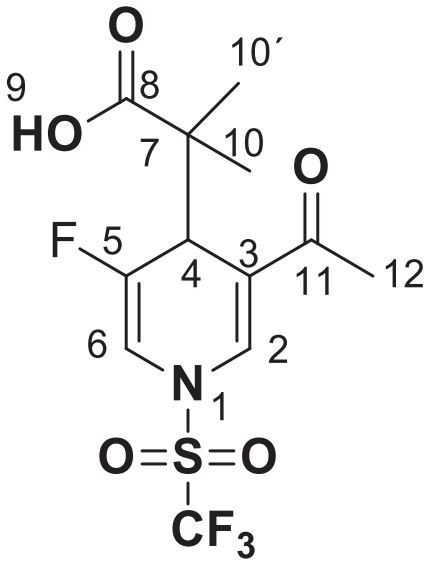

The compound was obtained as a white solid. mp. 122–124 °C, (0.37 g, 58%). IR ν_{max} KBr): 3097, 2978, 1705, 1661, 1203 cm^{-1}. ^1H NMR ($CDCl_3$, 300 MHz): $\delta = 7.49$ (s, 1H, H-2), 6.78 (d, $J = 4.8$ Hz, 1H, H-6), 4.31 (d, $J = 8.4$ Hz, 1H, H-4), 2.31 (s, H12, 3H, H-12), 1.18 (s, 3H, H-10), 1.00 (s, 3H, H-10′) ppm. ^{13}C NMR ($CDCl_3$, 75 MHz); $\delta = 195.1$, 179.6, 152.0, 149.4, 131.9, 122.6 (C6), 122.4 (C3), 119.1 ($J = 321.0$ Hz, CF_3), 117.4, 109.21, 46.3, 41.8, 25.4, 21.9, 21.3 ppm. HRMS: calcd for $C_{12}H_{14}F_4NO_5S$; calculated 360.0528, found 360.0532.

*4.3.5. 2-(3-acetyl-1-((trifluoromethyl)sulfonyl)-1,4-dihydroquinolin-4-yl)-2-methylpropanoic acid (**3e**)*

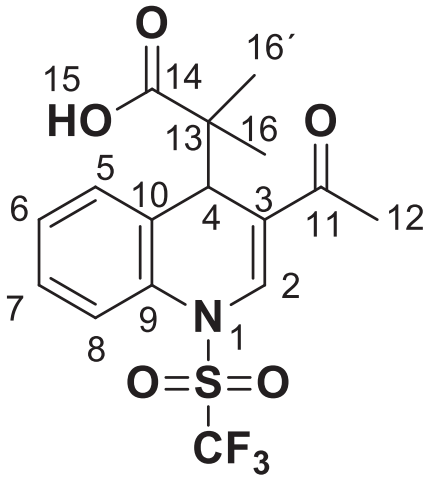

The compound was obtained as a white solid. mp. 140–144 °C, (0.21 g, 78%). IR ν_{max} (KBr): 2983, 1700, 1645, 1210 cm^{-1}. ^1H NMR ($CDCl_3$, 300 MHz): $\delta = 7.75$ (s, 1H, H-2), 7.62 (dd, $J = 8.5$, 1.5 Hz, 1H, H-7), 7.37-7.31 (m, 3H, H-5, H-6, H-8), 4.62 (d, $J = 0.9$ Hz, 1H, H-4), 2.45 (s, 1H, H-12), 1.10 (s, 3H, H-16) 1.09 (H-16′) ppm. ^{13}C NMR ($CDCl_3$, 75 MHz): δ = 195.3, 181.6, 135.8, 134.5, 131.1, 128.0, 127.4, 127.0, 126.2, 119.1 ($J = 321.0$ Hz, CF_3), 119.0, 49.1, 42.2, 25.2, 22.3, 20.9 ppm. HRMS: calcd for $C_{16}H_{17}F_3NO_5S$; calculated 392.0779, found 392.0711.

*4.3.6. 1-(3-acetyl-1-((trifluoromethyl)sulfonyl)-1,4-dihydropyridin-4-yl)cyclobutanecarboxylic acid (**3f**)*

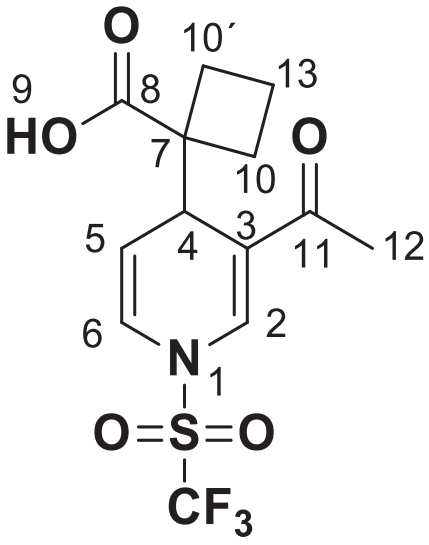

The compound was obtained as a white solid. mp. 78–80 °C, (0.37 g, 59%). IR ν_{max} (KBr): 3437, 2959, 1681, 1621, 1415, 1231 cm^{-1}. ^1H NMR ($CDCl_3$, 300 MHz): δ = 10.21 (s, 1H, H-9), 7.36 (s, 1H, H-2), 6.45 (d, J = 6.0 Hz, 1H, H-6), 5.25-5.20 (m, 1H, H-5), 3.83 (d, J = 6.0 Hz, 1H, H-4), 2.47 (s, 3H, H-12), 2.07-1.95 (m, 2H, H-10, H-10′), 1.73-1.68 (m, 2H, H-10′, H-10), 1.52-1.49 (m, 2H, H-13) ppm. ^{13}C NMR ($CDCl_3$, 75 MHz): δ = 196.5, 181.1, 132.3, 123.0, 122.3, 119.2 (J = 321.0 Hz, CF_3), 111.6, 53.5, 50.2, 28.4, 25.4, 23.0, 15.8 ppm. HRMS: calcd for $C_{13}H_{15}F_3NO_5S$ 354.0623, found 354.0650.

*4.3.7. 1-(3-acetyl-1-((trifluoromethyl)sulfonyl)-1,4-dihydropyridin-4-yl)cyclopentanecarboxylic acid (**3g**)*

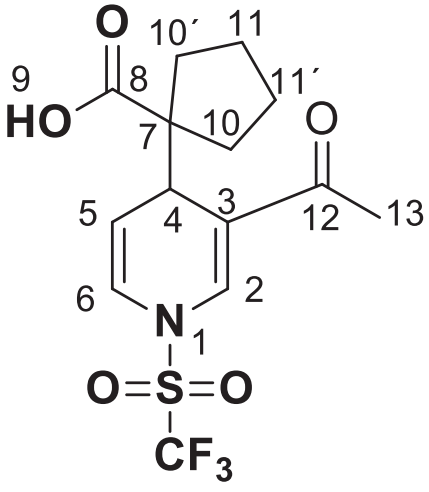

The compound was obtained as a white solid. mp. 58–60 °C, (0.31 g, 47%). IR ν_{max} (KBr). 3537, 2960, 1675, 1614, 1418, 1232 cm^{-1}. ^1H NMR ($CDCl_3$, 300 MHz): δ = 10.9 (s, H9), 7.26 (s, H2), 6.40 (d, J = 6.0 Hz, H6), 5.22-5.18 (m, H5), 3.84 (d, J = 6.0 Hz, H4), 2.10 (s, H13), 1.83-1.81 (m, H10'), 1.79-1.77 (m, H10), 1.34-1.30 (m, H11, H11') ppm. ^{13}C NMR ($CDCl_3$, 75 MHz): δ = 196.7, 181.8, 132.1, 123.1, 122.1, 119.2 (J = 321.0 Hz, CF_3), 112.6, 60.5, 50.3, 32.4, 31.9, 25.3, 23.8 ppm. DART$^+$-MS: 368 $[M+1]^+$, 350 $[M-18]^+$, 254 $[M-113]^+$ m/z. HRMS: calcd for $C_{14}H_{17}F_3NO_5S$ 368.0779, found 368.0802.

*4.3.8. 1-(3-acetyl-1-((trifluoromethyl)sulfonyl)-1,4-dihydropyridin-4-yl)cyclohexanecarboxylic acid (**3h**)*

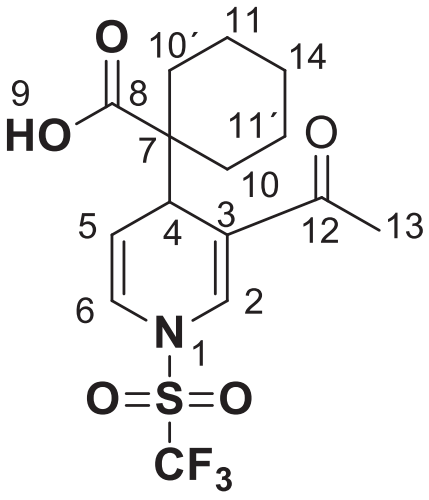

The compound was obtained as a white solid. mp. 162–164 °C, (0.48 g, 80%). IR ν_{max} (KBr): 3451, 2931, 1677, 1617, 1417, 1232 cm^{-1}. ^1H NMR ($CDCl_3$, 300 MHz): δ = 9.43 (s, 1H, H-9), 7.56 (s, 1H, H-2), 6.73 (d, J = 9.0 Hz, 1H, H-6), 5.47-5.43 (m, 1H, H-5), 3.94 (d, J = 6.0 Hz, 1H, H-4), 2.37 (s, 3H, H-13), 2.05-1.95 (t, J = 7.0 Hz, 2H, H-10, H-10′), 1.63 (t, J = 7.0 Hz, 2H, H-10′, H-10), 1.40-1.22 (m, 4H, H-11, H-11′), 1.09-0.92 (m, 2H, H-14) ppm. ^{13}C NMR ($CDCl_3$, 75 MHz): δ = 197.4, 180.4, 131.9, 122.6, 121.3, 119.1 (J = 321.0 Hz, CF_3), 111.8, 53.1, 38.8, 29.9, 29.7, 25.6, 25.3, 23.4, 23.3 ppm. HRMS: calcd for $C_{15}H_{19}F_3NO_5S$ 382.0936, found 382.0904.

*4.4. General procedure for the synthesis of dihydropyridine carboxylic acids **17a** and **17b***

To a solution of the corresponding alkyne **16a** or **16b** (1.76 mmol) dissolved in 15 mL of anhydrous CH_2Cl_2 (under an inert atmosphere and cooled to −78 °C), 0.36 mL (2.12 mmol, 1.2 equiv) triflic anhydride were added with a syringe and the mixture was stirred constantly for 3 h. Subsequently, 2.12 mmol (1.2 equiv) of the corresponding ketene acetal was added, followed by stirring at −78 °C for 2 h. The reaction was allowed to reach 25 °C, at which point it was transferred to a separatory funnel and washed with water (3 × 30 mL). The organic phases were combined and dried with anhydrous Na_2SO_4, and the solvent was removed by vacuum evaporation. The reaction crude was purified by column chromatography using silica gel with hexane/AcOEt mixtures as eluents to obtain **17a** and **17b**.

*4.4.1. 2-(3-(hex-1-yn-1-yl)-1-((trifluoromethyl)sulfonyl)-1,4-dihydropyridin-4-yl)-2-methylpropanoic acid (**17a**)*

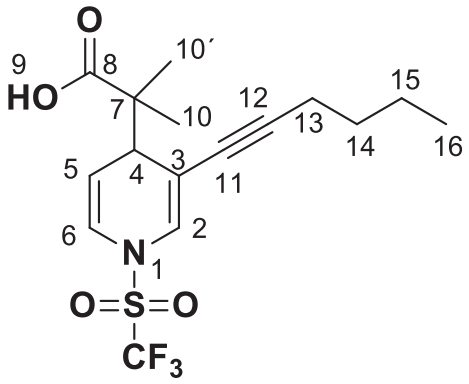

The compound was obtained as a white solid. mp. 136–138 °C, (0.36 g, 82%). IR ν_{max} (KBr): 3096, 2992, 2073, 1696, 1670, 1202 cm^{-1}. ^1H NMR ($CDCl_3$, 300 MHz): δ = 7.44-7.40 (m, 2H, H-14, H-14′), 7.36-7.32 (m, 3H, H-15, H-15′, H-16), 7.03 (s, 1H, H-2), 6.63 (d, J = 8.1 Hz, 1H, H-6), 5.14 (dd, J = 8.1, 5.1 Hz, 1H, H-5), 3.63 (d, J = 5.1 Hz, H4), 1.31 (s, 3H, H-10), 1.15 (s, 3H, H-10′) ppm. ^{13}C NMR ($CDCl_3$, 75 MHz) δ = 183.1, 131.4, 128.6, 128.4, 128.1, 122.7, 122.5, 119.4 (J = 324.3 Hz, CF_3), 109.6, 105.3, 90.8, 86.9, 47.4, 42.8, 21.7, 21.3 ppm. HRMS: calcd for $C_{18}H_{17}F_3NO_5S$; calculated 400.0830, found 400.0842.

4.5. General procedure for the synthesis of 2-(3-acetyl-1-((trifluoromethyl)sulfonyl)-1,4-dihydropyridin-4-yl)-2-methylpropanoic acid using D_2O

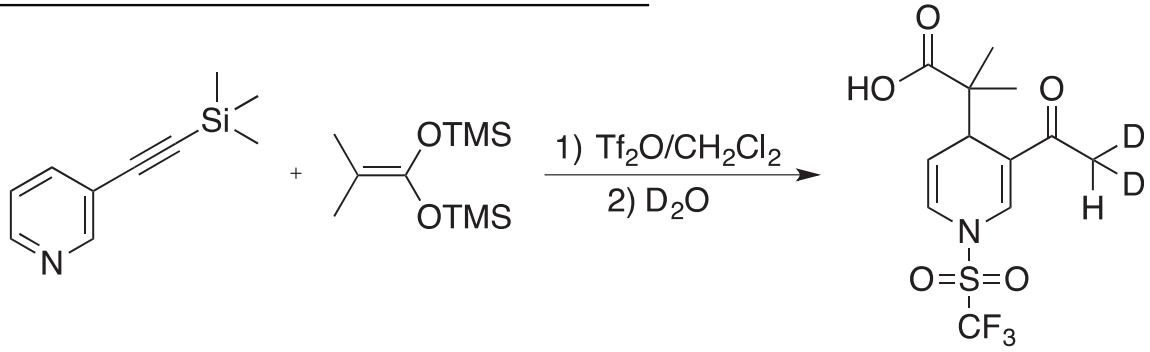

The compound was obtained as a white solid. mp. 124–126 °C, (0.31 g, 65%). IR ν_{max} (KBr): 3106, 2937, 2226, 1699, 1620 cm^{-1}. ^1H NMR ($CDCl_3$, 300 MHz): δ = 6.61 (s, 1H, H-2), 6.38 (dd. J = 8.2, 1.7 Hz, 1H, H-6), 4.93 (dd, J = 8.2, 5.0 Hz, 1H, H-5), 3.30 (d, J = 5.0 Hz, 1H, H-4), 2.02 (d, J = 6.9 Hz, 2H, H-13), 1.32-1.11 (m, 4H, H-14, H-15), 1.08 (s, 3H, H-10′), 0.95 (s, 3H, H-10), 0.69 (t, J = 6.9 Hz, 3H, H-16) ppm. ^{13}C NMR ($CDCl_3$, 75 MHz): δ = 183.0, 127.1, 122.7, 119.34 (J = 321.0 Hz, CF_3), 109.5, 105.9, 92.5, 78.0, 47.3, 42.9, 30.4, 22.1, 21.9, 21.3, 19.0, 13.6 ppm. HRMS: calcd for $C_{16}H_{21}F_3NO_4S$; calculated 380.1143, found 380.1101.

*4.4.2. 2-methyl-2-(3-(phenylethynyl)-1-((trifluoromethyl) sulfonyl)-1,4-dihydropyridin-4-yl)propanoic acid (**17b**)*

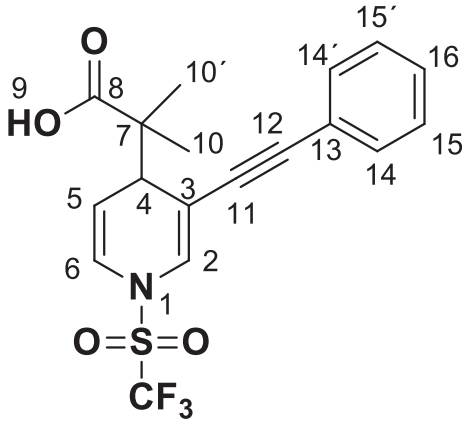

To a solution with 0.3g (1.76 mmol) 3-((trimethylsilyl)ethynyl) pyridine dissolved in 15 mL of anhydrous CH_2Cl_2 (under inert atmosphere and cooled to −78 °C), 0.36 mL (2.12 mmol, 1.2 equiv) of triflic anhydride were added with a syringe, and the mixture was stirred constantly for 3 h. Subsequently, 2.12 mmol (1.2 equiv) of the corresponding ketene acetal were added and stirring continued at −78 °C for 2 h. The reaction was then allowed to reach 25 °C. To this solution were added deuterium oxide 99.9 atom % D (D_2O). Then the reaction mixture was stirred (500 rpm) for 1h. The crude was transferred to a separating funnel and washed with water (3 × 30 mL). The organic phases were combined and dried with anhydrous Na_2SO_4, and the solvent was removed by vacuum evaporation. The reaction crude was purified by column chromatography using silica gel with hexane/AcOEt mixtures as eluents to obtain the title compounds.

The compound was obtained as a white solid. ^1H NMR ($CDCl_3$, 300 MHz); δ = 7.37 (s, 1H, H-2), 6.51 (q, J = 6.0 Hz, J = 1.2 Hz, 1H, H-6), 5.22 (q, J = 6.0 Hz, J = 4.5 Hz, 1H, H-5), 3.85 (d, J = 4.5 Hz, 1H, H-4), 2.16-2.12 (m, 1H, H-12), 0.92 (s, 3H, H-10′), 0.83 (s, 3H, H-10′) ppm. ^{13}C NMR ($CDCl_3$, 75 MHz); δ = 196.6, 181.7, 132.5, 122.8, 122.4, 119.1 (C, J = 321.0 Hz, CF_3), 111.6, 47.2, 37.7, 29.7, 20.9, 20.4 ppm; MHRMS: calcd for $C_{12}H_{15}F_3NO_5S$ 344.0622, found 344.0560.

4.6. General procedure for the synthesis of 2-(3-acetyl-1-((trifluoromethyl)sulfonyl)-1,4-dihydropyridin-4-yl)-2-methylpropanoic acid using CD_2Cl_2

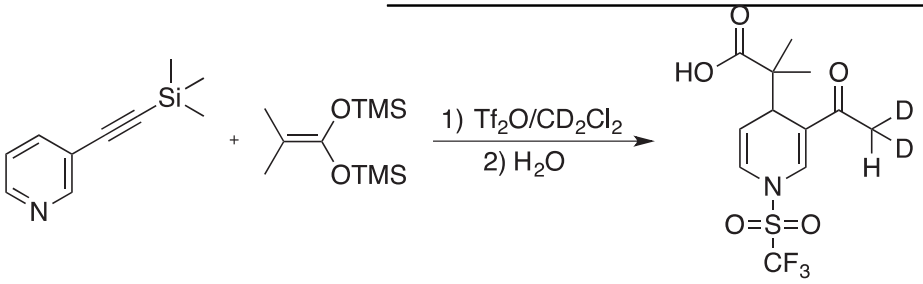

To a solution with 0.15 g (0.88 mmol) 3-((trimethylsilyl)ethynyl) pyridine dissolved in 7.5 mL of dichloromethane-d_2 99.9 atom % D (under inert atmosphere and cooled to −78 °C), 0.18 mL (1.06 mmol, 1.2 equiv) of triflic anhydride were added with a syringe, and the mixture was stirred constantly for 3 h. Subsequently, 1.06 mmol (1.2 equiv) of the corresponding ketene acetal were added and stirring continued at −78 °C for 2 h. The reaction was then allowed to reach 25 °C before being transferred to a separatory funnel and washed with water (3 × 15 mL). The organic phases were combined and dried with anhydrous Na_2SO_4, and the solvent was removed by vacuum evaporation. The reaction crude was purified by column chromatography using silica gel with hexane/AcOEt mixtures as eluents to obtain the title compound.

The compound was obtained as a white solid. ^{1}H NMR ($CDCl_3$, 300 MHz); $\delta = 7.39$ (s, 1H, H-2), 6.53 (q, $J = 6.0$ Hz, $J = 1.2$ Hz, 1H, H-6), 5.24 (q, $J = 6.0$ Hz, $J = 4.5$ Hz, 1H, H-5), 3.87 (d, $J = 6.0$ Hz, 1H, H-4), 1.09-1.06 (m, 1H-12), 0.94 (s, 3H, 10), 0.85 (s, 3H, H-10′) ppm. ^{13}C NMR ($CDCl_3$, 75 MHz); $\delta = 196.5$, 181.0, 132.5, 122.8, 122.4, 119.1 (C, $J = 321.0$ Hz, CF_3), 111.6, 47.2, 37.7, 31.6, 21.6, 20.4 ppm.; MHRMS: calcd for $C_{12}H_{12}D_3F_3NO_5S$ 345.0811, found 345.0560.

4.7. General procedure for the synthesis of 2-(3-acetyl-1-((trifluoromethyl)sulfonyl)-1,4-dihydropyridin-4-yl)-2-methylpropanoic acid using H_2O [18]

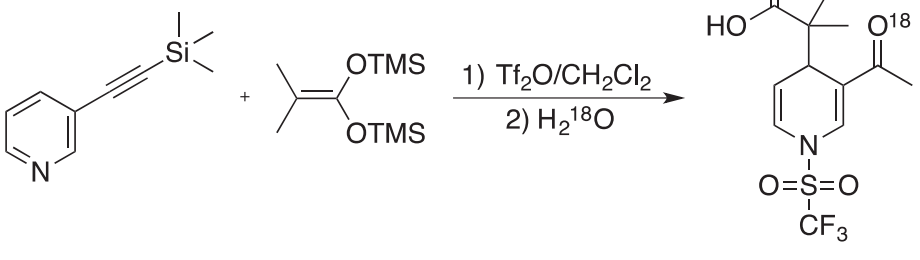

To a solution with 0.15 g (0.88 mmol) 3-((trimethylsilyl)ethynyl) pyridine dissolved in 7.5 mL of CH_2Cl_2 (under inert atmosphere and cooled to −78 °C), 0.18 mL (1.06 mmol, 1.2 equiv) of triflic anhydride were added with a syringe, and the mixture was stirred constantly for 3 h. Subsequently, 1.06 mmol (1.2 equiv) of the corresponding ketene acetal were added and stirring continued at −78 °C for 2 h. The reaction was then allowed to reach 25 °C. To this solution were added water-^{18}O 97 atom % ^{18}O (0.25 mL, $H_2^{18}O$). Then the reaction mixture was stirred (500 rpm) for 1h. The crude was transferred to a separating funnel and washed with water (3 × 30 mL). The organic phases were combined and dried with anhydrous Na_2SO_4, and the solvent was removed by vacuum evaporation. The reaction crude was purified by column chromatography using silica gel with hexane/AcOEt mixtures as eluents to obtain the title compounds.

The compound was obtained as a white solid. ^{1}H NMR ($CDCl_3$, 300 MHz); $\delta = 7.39$ (s, 1H, H-2), 6.53 (d, $J = 6.0$ Hz, 1H, H-5), 5.24 (q, $J = 5.7$ Hz, $J = 4.2$ Hz, 1H, H-5), 3.87 (d, $J = 4.2$ Hz, 1H, H-4), 2.18 (s, 3H, H-12), 0.93 (s, 3H, H-10), 0.85 (s, 3H, H-10′) ppm. ^{13}C NMR ($CDCl_3$, 75 MHz); $\delta = 196.5$, 181.5, 132.5, 122.8, 122.3, 119.2 ($J = 321.0$ Hz, CF_3), 111.6, 47.2, 37.8, 29.7, 21.5, 20.4 ppm; MHRMS: calcd for $C_{12}H_{12}D_3F_3NO_5S$ 344.06655, found 344.06546.

4.8. Analysis of the X-ray crystal structure of **3a**

Suitable X-ray quality crystals of **3a** were grown by slow evaporation from n-hexane/acetone solution at 4 °C. Details of the data collected and structure refinement parameters employed are summarized in Table 5.

4.9. Molecular docking

The dihydropyridine derivatives **3b**, **3e**, **17a** and **17b** as well as fluconazole were docked at the active site of the CYP51 enzymes of *C. albicans*, *C. dubliniensis*, *C. glabrata*, *C. krusei*, *C. lusitaniae* and *C. parapsilosis* on the AutoDock4 program [39]. The CYP51 enzymes of *Candida* spp. were previously modeled based on the crystallized CYP51 proteins of *C. glabrata* (PDB: 5JLC) and *C. albicans* (PDB: 5V5Z), deposited in the protein data bank (PDB) [40] as a template. To prepare the proteins, hydrogen atoms were added and water

Table 5
Crystal data and structure refinement for **3a**.

Empirical formula	$C_{12}H_{14}F_3NO_5S$
Formula wt ($g \cdot mol^{-1}$):	341.30
Crystal size (mm)	0.35 × 0.35 x 0.34
Color	Colourless
Crystal system	Monoclinic
Space group	$P2_1/c$
a (Å)	12.021(2)
b (Å)	9.911(2)
c (Å)	13.838(3)
α (°)	90
β (°)	106.59
γ (°)	90
V (Å^3)	1580.2(6)
Z	4
D_{calcd}(g/cm^3)	1.435
No. of reflections collected	3419
No. of independent reflections (Rint)	3419
Maximum and minimum transmission	0.746 and 0.611
Data/parameters	3419/207
Goodness-of-fit on F	1.019

molecules around the proteins removed before optimization on the Nanoscale Molecular Dynamics (NAMD) program [41].

The test compounds and reference drug were drawn on ChemBioDraw Ultra 12.0 software [42], converted to 3D with the Open Babel GUI program [43] and optimized with GaussView 6.0 software, involving the addition of hydrogen atoms and a check of the bond lengths and angles. The docking parameters were examined with AutoDock Tools (ADT), adopting a grid box of 48 × 42 × 40 Å^3 and points separated by 0.375 Å. The grid center values were established for each CYP51 enzyme: X = −47,731, Y = −13,422 and Z = 22,982 for the CYP51 of *C. albicans*; X = −43,598, Y = −13,588 and Z = 25,836 for the CYP51 of *C. dubliniensis*; X = −31,107, Y = 68,515 and Z = −21,415 for the CYP51 of *C. glabrata*; X = −43,311, Y = −9941 and Z = 25,384 for the CYP51 of *C. krusei* and *C. lusitaniae*; X = −45,446, Y = −10.26 1 and Z = 22,645 for the CYP51 of *C. parapsilosis*. The Lamarckian genetic algorithm was employed, performing a total of 100 docking runs. The docked model with the lowest binding energy was considered. The docking results were edited with Discovery Studio client [44].

4.10. Evaluation of antifungal activity

The *in vitro* inhibition produced by fluconazole and four dihydropyridine derivatives was determined on six *Candida* species (*C. albicans*, *C. dubliniensis*, *C. glabrata*, *C. krusei*, *C. lusitaniae* and *C. parapsilosis*), using the guidelines recommended by the National Committee for Clinical Laboratory Standards (NCCLS). The test medium was RPMI 1640 buffered with 0.165 MMOPS (both from Sigma) [45]. The MIC value was defined as the lowest concentration of the dihydropyridine derivatives that afforded a culture with a reading of turbidity indicating 100% inhibition when compared to the growth of the control. The dihydropyridine derivatives were dissolved in DMSO and serially dripped onto the growth medium. The concentrations gradients utilized were 64−0.0325 μg/mL for fluconazole and 160−0.078125 μg/mL for **3b**, **3e**, **17a** and **17b**. The inoculum was prepared with colonies from a yeast culture at 24 h of growth, resuspended in a saline solution (0.85% NaCl) and adjusted to an optical density of 0.5 McFarland. Subsequently, they were incubated at 37 °C durin 24 h. After agitation of the plates, the MIC values were ascertained in a Multiskan ™ GO microplate spectrophotometer with the reading taken at a wavelength of 450 nm. The value presently reported is the average of three experiments.

Funding

The authors wish to thank Maria del Rocio Patiño-Maya for technical support. The authors gratefully acknowledge the financial support of CONACYT-México, under the Project Number 252020, and the DGAPA-PAPIIT Project Number IN203120. JOGG and DMAP acknowledges financial support from the SIP-IPN, Project Number 20200950.

Declaration of competing interest

The authors declare that they have no known competing financial interests or personal relationships that could appear to influence the work reported in this paper.

Acknowledgments

The authors would like to thank Miguel A. Sierra Rodriguez and Bruce Allan Larsen for proofreading the manuscript.

Appendix A. Supplementary data

Supplementary data to this article can be found online at https://doi.org/10.1016/j.tet.2021.132086.

References

[1] U.S. Schubert, C. Eschbaumer, Org. Lett. 1 (1999) 1027−1029.
[2] O. Gómez-García, E. Gomez, R.A. Toscano, H. Salgado-Zamora, C. Álvarez-Toledano, Synthesis 48 (2016) 1371−1380.
[3] R. Toscano, R. Rosas, M. Hernández-Galindo, del Cármen, C. Alvarez-Toledano, O. Garcia-Mellado, Transit. Met. Chem. 23 (1998) 113−116.
[4] T. Itoh, M. Miyazaki, K. Nagata, A. Ohsawa, Heterocycles (1997) 83−86.
[5] A. Rivera-Hernández, G.M. Chans, H. Rudler, J.G.L. Cortés, R.A. Toscano, C. Álvarez-Toledano, Tetrahedron 70 (2014) 1861−1871.
[6] Y. Xu, E. Aldeco-Pérez, H. Rudler, A. Parlier, C. Alvarez, Tetrahedron Lett. 47 (2006) 4553−4556.
[7] A. Parlier, C. Kadouri-Puchot, S. Beaupierre, N. Jarosz, H. Rudler, L. Hamon, P. Herson, J. Daran, Tetrahedron Lett. 50 (2009) 7274−7279.
[8] E. Ullah, S. Rotzoll, A. Schmidt, D. Michalik, P. Langer, Tetrahedron Lett. 46 (2005) 8997−8999.
[9] L. Ostrosky-Zeichner, J. Sobel, Fungal infections, Infect. Dis. Clin. 30 (2016) 1−313.
[10] G. Suleyman, Alangaden, Infect. Dis. Clin. 30 (2016) 1023−1052.
[11] S.R. Lockhart, J. Guarner, Semin. Diagn. Pathol. 36 (2019) 177−181.
[12] V. Krcmery, A. Barnes, J. Hosp. Infect. 50 (2002) 243−260.
[13] S. Campoy, J.L. Adrio, Biochem. Pharmacol. 133 (2017) 86−96.
[14] A. Du Toit, Nat. Rev. Microbiol. 15 (2017), 1-1.
[15] R.H. Jensen, Dan Med. J. 63 (2016) 1−34.
[16] Z. Ježíková, T. Pagáč, B. Pfeiferová, H. Bujdáková, S. Dižová, I. Jančíková, D. Gášková, P. Olejníková, Antonie Leeuwenhoek 110 (2017) 1219−1226.
[17] D.M. Patel, M.G. Sharma, R.M. Vala, I. Lagunes, A. Puerta, J.M. Padrón, D.P. Rajani, H.M. Patel, Bioorg. Chem. 86 (2019) 137−150.
[18] A.A. Altaf, A. Shahzad, Z. Gul, N. Rasool, A. Badshah, B. Lal, E.J. Khan, Drug Des. Med. Chem. 1 (2015) 1−11.
[19] A. Moran, E. Martín, C. Velasco, M.L. Martín, L.S. Roman, E. Caballero, P. Puebla, M. Medarne, A.S. Feliciano, J. Pharm. Pharmacol. 49 (1997) 421−425.
[20] V. Onnis, M.T. Cocco, R. Fadda, C. Congiu, Bioorg. Med. Chem. 17 (2009) 6158−6165.
[21] T. Sakamoto, Y. Kondo, M. Shiraiwa, H. Yamanaka, Synthesis (1984) 245−247.
[22] F. Li, N. Wang, L. Lu, G. Zhu, J. Org. Chem. 80 (2015) 3538−3546.
[23] A.K. Das, S. Park, S. Muthaiah, S. Hong, Synlett 26 (2015) 2517−2520.
[24] S. Liang, J. Jasinski, G.B. Hammond, B. Xu, Org. Lett. 17 (2015) 162−165.
[25] W. Baidossi, M. Lahav, J. Blum, J. Org. Chem. 62 (1997) 669−672.
[26] X. Jin, T. Oishi, K. Yamaguchi, N. Mizuno, Chem. A Eur J. 17 (2011) 1261−1267.
[27] C.M. Yates, E.P. Garvey, S.R. Shaver, R.J. Schotzinger, W.J. Hoekstra, Bioorg. Med. Chem. Lett 27 (2017) 3243−3248.
[28] X. Che, C. Sheng, W. Wang, Y. Cao, Y. Xu, H. Ji, G. Dong, Z. Miao, J. Yao, W. Zhang, Eur. J. Med. Chem. 44 (2009) 4218−4226.
[29] O. Gómez-García, D. Andrade-Pavón, E. Campos-Aldrete, R. Ballinas-Indilí, A. Méndez-Tenorio, L. Villa-Tanaca, C. Álvarez-Toledano, Molecules 23 (2018) 599.
[30] A.K. Chhillar, P. Arya, C. Mukherjee, P. Kumar, Y. Yadav, A.K. Sharma, V. Yadav, J. Gupta, R. Dabur, H.N. Jha, Bioorg. Med. Chem. 14 (2006) 973−981.
[31] Z. Ježíková, T. Pagáč, B. Pfeiferová, H. Bujdáková, S. Dižová, I. Jančíková, D. Gášková, P. Olejníková, Antonie Leeuwenhoek 110 (2017) 1219−1226.

[32] H. Niaz, H. Kashtoh, J.A. Khan, A. Khan, M.T. Alam, K.M. Khan, S. Perveen, M.I. Choudhary, Eur. J. Med. Chem. 95 (2015) 199–209.
[33] D.M. Patel, M.G. Sharma, R.M. Vala, I. Lagunes, A. Puerta, J.M. Padrón, D.P. Rajani, H.M. Patel, Bioorg. Chem. 86 (2019) 137–150.
[34] H.M. Refat, A. Fadda, Eur. J. Med. Chem. 70 (2013) 419–426.
[35] M. Sharma, D. Rajani, H.R. Patel, Soc. Open Sci. 4 (2017) 170006.
[36] G. Yang, X. Shang, P. Cheng, X. Yin, J. Zhu, Y. Liu, J. Zhang, Z. Zhang, Molecules 23 (2018) 2422.
[37] C. Ainsworth, Y. Kuo, J. Organomet. Chem. 46 (1972) 73–87.
[38] Y. Lei, T. Hu, X. Wu, Y. Wu, H. Xiang, H. Sun, Q. You, X. Zhang, Tetrahedron Lett. 57 (2016) 1100–1103.
[39] G.M. Morris, R. Huey, W. Lindstrom, M.F. Sanner, R.K. Belew, D.S. Goodsell, A.J. Olson, J. Comput. Chem. 30 (2009) 2785–2791.
[40] H.M. Berman, J. Westbrook, Z. Feng, G. Gilliland, T.N. Bhat, H. Weissig, I.N. Shindyalov, P.E. Bourne, Nucleic Acids Res. 28 (2000) 235–242.
[41] J.C. Phillips, R. Braun, W. Wang, J. Gumbart, E. Tajkhorshid, E. Villa, C. Chipot, R.D. Skeel, L. Kale, K. Schulten, J. Comput. Chem. 26 (2005) 1781–1802.
[42] K.R. Cousins, J. Am. Chem. Soc. 133 (2011) 8388.
[43] N.M. O'Boyle, M. Banck, C.A. James, C. Morley, T. Vandermeersch, G.R. Hutchison, J. Cheminf. 3 (2011) 33.
[44] Dassault Systèmes BIOVIA, Discovery Studio Modeling Environment; Release 2017, Dassault Systèmes, San Diego, CA, USA, 2016.
[45] M. Cuenca-Estrella, W. Lee-Yang, M.A. Ciblak, B.A. Arthington-Skaggs, E. Mellado, D.W. Warnock, J.L. Rodríguez-Tudela, Antimicrob. Agents Chemother. 46 (2002) 3644–3647.